IRSTI 41.23.15; 41.23.17 https://doi.org/10.26577/phst20251215

Method for determining the physical parameters of hot supergiants based on spectral energy distribution analysis

A.T. Gyuchtash [1], Sh.T. Nurmakhametova[1], N.L. Vaidman[1], S.A. Khokhlov, A.T. Agishev[1*] and A. Bakhytkyzy[2]

[1]Fesenkov Astrophysical Institute, Observatory, Almaty, Kazakhstan
[2]Department of Physics and Astronomy, University of North Carolina – Greensboro, Greensboro, NC, USA
*e-mail: Aldiyar.Agishev@gmail.com
(Received April 25, 2025; received in revised form May 23, 2025; accepted June 3, 2025)

This study determines the physical parameters of B- and A-type hot supergiants through the construction and analysis of their spectral energy distributions (SEDs). These luminous stars are in the late stages of stellar evolution and are important for understanding stellar structure and the chemical evolution of galaxies. Although previous spectroscopic studies provided extensive information, our application of the comprehensive SED analysis represents a novel approach to further refine and validate these parameters. We refined the effective temperature Teff, surface gravity (log g), and interstellar extinction A_V for a sample of 16 supergiants using multiwavelength photometry spanning from the ultraviolet to the infrared. A dedicated software package written in Fortran was used to convert observed magnitudes into physical fluxes and compare them with synthetic photometry derived from Castelli & Kurucz model atmospheres. The optimal parameter set for each star was obtained by minimizing the deviations between the observed and model SEDs, iterating over A_V values. The resulting parameters show good agreement with those published in the literature, confirming the reliability of our approach.

Key words: supergiants, spectral energy distribution, interstellar extinction, effective temperature, surface gravity.
PACS number(s): 97.20.Pm, 97.10.Ex

1 Introduction

Hot supergiants are stars in the late stages of their evolution. They can serve as standard candles to measure extragalactic distances and are important for understanding stellar evolution processes. One of the most effective tools for studying such objects is the construction of spectral energy distributions (SED), which allows us to accurately determine their physical parameters, such as the effective temperature (Teff), surface gravity (log(g)), and interstellar reddening (Av).

The choice of this research topic is due to the need for a deeper understanding of the physics of hot supergiants. Despite significant progress in astronomy, their fundamental parameters remain poorly understood and are not well-constrained. Numerous studies, such as those by [1], [2] and [3], have made a huge contribution to the study of hot supergiants, but there is still a lack of comprehensive studies covering a wide range of such stars, which emphasizes the relevance of this project.

Although previous spectroscopic studies provided extensive information, our application of comprehensive SED analysis represents a novel approach to further refine and validate these parameters.

The aim of the present study is to use the SED construction method to determine the parameters of hot B-A supergiants. The objectives of the study include constructing the SED for 16 stars, analyzing their spectral data, and applying extrapolation and modeling methods to refine the values of Teff, log(g), and Av. Selected stars span a temperature range from 8 000 to 13 000 K, which provides good coverage of the main types of hot supergiants (spectral classes B and A). This makes the sample representative in terms of physical diversity and suitable for testing the method. Moreover, selected stars are the most interesting and intriguing ones investigated earlier. The SED-method was never

used for them before, though different spectroscopic methods were used, so our investigation is very representative for this sample of objects. In addition, all selected stars have reliable multi-band photometric data, which is essential for constructing accurate SED.

We will compare our derived parameters with previously obtained values from other studies to assess the accuracy and consistency of our results. This comparison will help to confirm the reliability of our methods and provide a broader context for the physical parameters of hot supergiants. By comparing our results with those from established studies, we aim to identify any discrepancies or confirm the results, thereby contributing to a more accurate understanding of the stellar characteristics of the selected supergiants.

The methods used in this study include the use of modern astronomical databases and tools for analyzing observational data, such as tools for constructing and analyzing SEDs, as well as statistical methods for data processing, including optimization methods for fitting models. The approach proposed in the paper is based on the use of new data, which significantly improves the accuracy of determining the parameters of supergiants.

The theoretical significance of the work lies in improving the methods for determining the physical parameters of hot supergiants and expanding knowledge about the processes occurring in stars at late stages of their evolution. The practical significance lies in the possibility of using the obtained data to refine the models of stellar evolution and applying the SED method to the study of other types of stars.

Literature review

HD 87737. HD 87737 is classified as an A0 Ib supergiant and has been extensively studied to determine its fundamental parameters. Teff = 10 400 ± 300 K and log(g) = 2.05 ± 0.20 were reported [4]. Two options for the effective temperature were given as Teff = 9 460 / 8 920 K [5], while Teff = 9 400 K was estimated [6]. A higher estimate of Teff = 10 500 K and log(g) = 2.2 was provided [7]. Teff was refined to 10 200 ± 370 K, with log(g) = 1.9 ± 0.4 [8]. Teff = 9 650 ± 200 K and log(g) = 1.95 ± 0.10 were derived based on the ionization equilibrium of Mg I/Mg II [9].

Earlier works contributed to the understanding of HD 87737's parameters. Initial evaluations of equivalent widths of spectral lines were provided [10, 11], and using these values, the parameters were recalculated by [3], resulting in Teff = 9 500 K and log(g) = 1.1, and Teff = 9 300 K and log(g) = 0.9. Then, in [3] new data was used to derive Teff = 9 700 K and log(g) = 2.0.

Subsequent studies reported slightly different values. Teff = 9 600 ± 150 K and log(g) = 2.00 ± 0.15 were derived [12], and Teff = 9 730 K and log(g) = 1.97 were estimated using the MILES spectral library [13]. Teff = 9 820 ± 340 K and E(B–V) = 0.053 were provided [14]. Later, Teff = 9 600 ± 150 K and log(g) = 2.00 ± 0.10 were reported [15], and Teff = 9,600 ± 200 K and log(g) = 2.05 ± 0.10 with E(B-V) = 0.02 ± 0.02 were determined [1]. Thus, HD 87737 has been studied extensively over the years, providing a wide range of determined fundamental parameters.

HD 46300. HD 46300 is a supergiant, classified as an A0 Ib, which has been studied several times through years. In [5] two evaluations for the effective temperature are derived, Teff = 8 940 / 8 800 K. In [4] Teff is determined to be 9 800 ± 200 K, with log(g) = 2.15 ± 0.10. As for HD 87737, initial estimates provided by [10] and [11] were recalculated, and in the follow-up work in [3] obtained Teff = 9 500 K and log(g) = 1.0 for [10] and Teff = 9700 K and log(g) = 1.5 for [11]. Using her own data, [3] refined the parameters of her previous work to Teff = 9 700 K and log(g) = 2.1.

The parameters were then refined by further studies, such as in [2], who derived Teff = 9 750 K and log(g) = 2.0. In [2] it is also noted that in [16] T_{eff} equals 9 730 K. Then, [14] estimated Teff = 9 800 ± 340 K and E(B-V) = 0.083. More recently, [1] reported Teff = 11 000 ± 200 K and log(g) = 2.15 ± 0.10, with E(B–V) = 0.07 ± 0.02.

BD +60 2582. BD +60 2582 is a supergiant classified as a B7 Iab. It was studied mainly by [1], who reported Teff = 11 900 ± 200 K and log(g) = 1.85 ± 0.10 using spectroscopic data and refined model atmospheres. Additionally, they estimated E(B–V) = 0.85 ± 0.02, which nearly corresponds to the previous measurement by [17], who obtained an evaluation for the interstellar reddening A_V = 2.34.

HD 5776. HD 5776 is classified as an A2 Iab supergiant. [17] estimated the interstellar reddening as A_V = 1.53. Fundamental parameters of the star were reported by [18], who derived Teff = 10 715 K based on spectroscopic analysis. Later, [2] provided a lower temperature estimate of Teff = 9 500 K and log(g) = 1.0. In this paper it is also noted that the estimation given by [16] is T_{eff} = 9730.

BD +61 153. BD +61 153 is classified as an A2 Iab supergiant, which was not studied a lot as well. [17] obtained A_V = 2.49. Fundamental parameters of the star were determined by [2], who provided the effective temperature Teff = 9 750 K and log(g) = 1.5. Moreover, in [2] the effective temperature was noted, which was estimated by [16].

HD 161695. HD 161695 is classified as an A0 Ib supergiant. According to the [13], it has an effective temperature of Teff = 9 950 K and a surface gravity of log(g) = 2.2. These values were included in MILES stellar library.

HD 175687. HD 175687 is classified as a B9/A0 Ib supergiant. In [3], the effective temperature for HD 175687 was calculated to be Teff = 9 400 K, with log(g) = 2.3. These parameters were obtained by observing hydrogen line profiles and using ionization equilibrium.

HD 16778. HD 16778, classified as an A1 Ia supergiant, was studied by [18], who estimated its effective temperature Teff to be 9 550 K. This estimate was derived from the spectroscopic analysis.

HD 202850. HD 202850 is classified as a B9 Iab supergiant and was studied several times. In [19] determined Teff = 11 000 K and log(g) = 1.87. In [20] derived an estimate for the interstellar reddening, reporting E(B–V) = 0.13, Further studies, such as [14], estimated Teff = 11 170 ± 450 K and reported E(B–V) = 0.2. In [15] and [1] consistently reported Teff = 10 800 ± 200 K and log(g) = 1.85 ± 0.10, with E(B–V) values of 0.19 ± 0.02.

HD 40589. HD 40589 is classified as an A0 Iab supergiant. It was studied by [21], who determined Teff = 12 000 and log(g) = 1.8. Later, in [14] estimated the effective temperature of HD 40589 to be Teff = 11 660 ± 490 K, based on atmospheric modeling and comparisons with observed photometric data. In [22] the parameters for this star were refined, reporting Teff = 10 750 ± 150 K and log(g) = 1.65 ± 0.2, using a combination of atmospheric models and the parallax method.

HD 46769. HD 46769, classified as a B7 Ib supergiant, has been studied in several key works. In [23], the effective temperature was estimated to be Teff = 12 000 K, with surface gravity values of log(g) = 2.57. In [14] derived Teff = 13 920 ± 710 K, along with E(B–V) = 0.151, which provides a more refined temperature estimate along with a better understanding of the reddening effect for the star. In [24] the parameters were refined further, reporting Teff = 13 000 ± 1 000 K and log(g) = 2.7 ± 0.1.

HD 59612. HD 59612, classified as an A5/7 Iab/II supergiant, has been studied by [3], who estimated Teff = 8 100 K and log(g) = 1.45, based on spectroscopic data and model fitting. In [2] the parameters were refined to Teff = 8 500 K and log(g) = 1.5. Additionally it is noted that in [16] T_{eff} = 8 510 K is received. In [13] Teff = 8 330 K and log(g) = 1.45 is estimated, and in [25] Teff = 8 620 K and log(g) = 1.78 is reported.

HD 67456. HD 67456, classified as an A3 Ib/II supergiant, has been studied mainly by [26], who provided initial estimates, which were recalculated by [3] based on previous measurements of equivalent widths. In [3] the effective temperature for HD 67456 is derived as Teff = 9 500 K and log(g) = 1.2. In [3] the parameters for HD 67456 were recalculated using new data, reporting Teff = 8 300 K and log(g) = 2.5, which is noticeably lower than those from earlier estimates.

HD 71833. HD 71833, classified as a B8 II supergiant, was studied by [27], who determined its effective temperature to be Teff = 12 985 K using the calibration of Strömgren photometric parameters [28].

HD 35600. HD 35600 is classified as a B9 Ib supergiant. In [29] Teff = 11 500 K and log(g) = 2.10 are reported, based on spectroscopic analysis and model fitting. Later, in [21] the parameters were refined, estimating Teff = 11 000 K and log(g) = 1.9.

HD 212593. HD 212593, classified as a B9 Iab-Ib supergiant, has been extensively studied. Early estimates [6] provided Teff = 9 932 K, followed by [2] with Teff = 10 000 K and log(g) = 1.5. It is also noted that in [16] T_{eff} = 10 300 K is estimated. Later studies refined these values, with Teff = 10 350 K and log(g) = 1.92 [30], and in [19] a higher estimate of Teff = 11 800 K and log(g) = 2.19 is provided.

Subsequent studies, including [15] and [1], consistently reported Teff = 11 200 ± 200 K and log(g) = 2.10 ± 0.10, with E(B–V) = 0.17 ± 0.02. In [14] Teff = 11 150 ± 440 K is estimated, and in [31] E(B–V) = 0.120 is confirmed. In [32], the most recent study, the effective temperature was derived as Teff = 13 642 K with log(g) = 3.00.

2 Materials and methods

To assemble the SED for the selected stars, we collected photometric measurements spanning a wide wavelength range–from the ultraviolet through the far-infrared. These data were sourced from

several major catalogs available via the Vizier service [33] and the General Catalogue of Photometric Data (GCPD) [34], covering various photometric systems.

For the ultraviolet region, we used measurements from the TD1 space survey [35], which provides fluxes in four bands centered at 1565, 1965, 2365, and 2740 Å. These observations were obtained with the ultraviolet telescope aboard the ESRO satellite.

In the optical range, photometry in the Johnson UBVRI system [36] formed the core dataset. This was complemented by data in the Strömgren uvby system, drawn from both earlier [37] and recent [38] observations. When available, the color indices m1 and c1 were used to reconstruct individual filter magnitudes algorithmically within the input format of our SED-processing tool.

Near-infrared data were taken from the 2MASS catalog by [39], which includes the J, H, and K bands. To account for possible saturation effects in very bright sources, especially in the K band, we additionally included fluxes from the pre-1999 CIO catalog [40].

At longer wavelengths, we incorporated mid- and far-infrared data from the WISE mission [41]. The four WISE bands – W1 (3.4 μm), W2 (4.5 μm), W3 (11.6 μm), and W4 (22 μm) – provided high-precision photometry across the entire sample, within the survey's brightness limits.

Supplementary photometric measurements in the UBV, Strömgren, and JHK systems were also obtained from the GCPD to ensure consistency and maximize coverage across filters.

In cases where the input file included the letter "J" after the spectral classification, this denoted that the V−R and R−I color indices were specified in the Johnson photometric system. If, instead, the file contained the symbol "N", it indicated that these measurements were not provided. Once the full set of available magnitudes was assembled, each value was converted into an absolute flux using standard zero-points based on the flux calibration of Vega (i.e., corresponding to magnitudes of zero), together with the transmission profiles of the relevant filters.

While systematic catalog offsets were not explicitly corrected within the software, careful pre-selection and manual vetting of the photometric data minimized potential biases.

To determine stellar parameters from photometric data, we developed a custom software suite written in Fortran. It comprises three main modules, each responsible for a distinct stage of the parameter estimation process, which together form a complete optimization pipeline.

The first module preprocesses the input spectra from the Castelli-Kurucz model [42] grid by trimming them to the relevant wavelength range, converting flux units as needed, and applying normalization – typically with respect to the V-band–to ensure numerical stability during further analysis.

The second module performs synthetic photometry by convolving the normalized spectra with the transmission curves of the selected filters. The resulting integrated fluxes are then converted to synthetic magnitudes using standard zero-points, providing a direct comparison to the observed photometric data.

The final module performs the core fitting and optimization. It loads the observed multi-band magnitudes, converts them into physical fluxes, and applies interstellar extinction to each trial model while systematically varying Teff, log(g), and Av. For every combination of parameters, the program evaluates how well the model matches the observed data and selects the best fitting set by minimizing the deviation. The output includes the derived physical parameters along with visual diagnostic plots comparing models to observations.

Because photometric observations are usually expressed in magnitudes, which follow a logarithmic scale, the data are first converted to linear flux units using the standard relation:

$$F_\lambda = F_0 \times 10^{-0.4m} \quad (1)$$

where F_λ– observed flux at wavelength λ; F_0 – reference (zero-point) flux corresponding to m=0; m – stellar magnitude in the given photometric band.

However, the absolute flux level of the observed SED depends not only on the star's effective temperature and surface gravity, but also on its radius and distance, which are generally unknown or not constrained in photometric fitting. Therefore, the model SED is normalized to match the observed flux in a reference band (typically the V band), and the comparison is performed in relative units. As a result, the absolute scaling of the SED is not fixed during the fitting process.

Instead, the fitting process focuses on the relative shape of the SED. Both the observed and model fluxes are normalized to a reference photometric band – typically the V-band in the

optical – so that their overall levels match. In effect, the model is scaled to align with the observed flux in that band. This removes the dependence on distance and stellar size, allowing a direct comparison of the SED profiles. Only the relative differences in flux across wavelengths – driven by Teff, log(g), and Av–are considered, while absolute offsets are intentionally ignored.

Our calculations rely on a grid of model stellar spectra computed by Castelli and Kurucz [42], which provide theoretical flux distributions as functions of wavelength, parameterized by effective temperature Teff, log(g), and chemical composition. In this study, we used a broad range of models covering temperatures from approximately 3500 K to 50,000 K and surface gravities from log(g) = 0.0 to 5.0 (in cgs units), making it possible to model a wide variety of stars–from cool supergiants to hot main-sequence stars. Unless otherwise specified, solar metallicity was assumed, although adjustments can be made if the chemical composition of the target star is known.

The model spectra used in this study are provided at a sufficiently high spectral resolution to ensure accurate integration across broad photometric passbands. In the first module, each spectrum is processed to match the requirements of the filter set: it is interpolated or truncated as necessary to cover the relevant wavelength range and may be smoothed or resampled depending on the task. The spectra can also be normalized – for example, to the bolometric flux or the flux in a specific photometric band – to facilitate comparison with observational data.

Since the original models are computed in absolute physical units (erg cm^{-2} s^{-1} $Å^{-1}$) at the stellar surface, a direct comparison with observational fluxes – which are distance-dependent – would require conversion to apparent fluxes received at Earth. In practice, however, such comparisons focus on the relative shape of the SED, not on its absolute level. To this end, both model and observed fluxes are scaled to a common reference, typically the V band, effectively removing the dependence on distance and stellar radius.

Synthetic photometry is then generated by convolving the model spectrum with the response curves of the selected filters. The resulting fluxes are converted to magnitudes using the adopted photometric zero-points, making them directly comparable with the observed photometric data.

In the final stage, the fitting and optimization module (final module) compares the observed and synthetic SEDs to determine the best-fit stellar parameters. Observed magnitudes are first converted into physical fluxes and normalized. For each trial model (i.e., a combination of Teff and log(g)) , the program iteratively applies interstellar extinction for a range of A_V values using an extinction law [43] (2) adjusts the model SED accordingly, and calculates the deviation from the observed SED.

$$F_\lambda^{dered} = F_\lambda^{obs} \times 10^{0.4A(\lambda)} \quad (2)$$

where F_λ^{dered}– de-reddened (intrinsic) flux at wavelength λ; F_λ^{obs} – observed flux at wavelength λ; A(λ) – total extinction at wavelength, given by $A(\lambda)=A_V k(\lambda)$, k(λ) – extinction curve normalized to A_V (e.g., [43]).

The deviation is quantified using a weighted relative deviation metric σ, which is calculated from the relative difference between the de-reddened observed and model fluxes, weighted by the inverse squared photometric uncertainties:

$$\sigma = \sqrt{\frac{1}{N-1}\sum_{i=1}^{N} \left(1 - \frac{F_{\lambda,i}^{dered}}{F_{\lambda,i}^{mod}}\right)^2 \times \omega_i} \quad (3)$$

where σ – weighted standard deviation of the relative residuals; $F_{\lambda,i}^{dered}$– de-reddened observed flux at wavelength λ_i; $F_{\lambda,i}^{mod}$– model flux at wavelength λ_i; $\omega_i = 1/\sigma_i^2$ – weight factor based on the squared photometric uncertainty σ_i; N – number of photometric data points used in the comparison. Outliers were identified based on significant deviations from the model or large photometric errors, with thresholds applied manually based on data quality and visual inspection. The optimization process is repeated over the entire model grid to find the minimum σ value.

The parameter set that yields the lowest deviation is adopted as the best solution. The parameter set that yields the lowest deviation is adopted as the best solution. Sensitivity to initial parameter guesses is not evaluated, as the selection is performed via full-grid search. However, sensitivity to extinction A_V is indirectly accounted for through the sampling density and range defined in the input grid, though no formal stability analysis of the solutions is performed. If required, the code also examines how sensitive the solution is to

changes in the parameters and whether other minima exist nearby.

The program outputs the optimal physical parameters – Teff, log(g), and A_V – as well as the corresponding model SED expressed in logarithmic form: log(λ), log (λFλ / λνFν), suitable for SED visualization. This allows not only a quantitative comparison with observational data, but also a visual assessment of the fit. Deviations in the infrared, for instance, may signal the presence of excess emission from circumstellar dust.

Although our method generally yields effective temperatures and extinction values that are in good agreement with the literature, the derived surface gravities for some stars are noticeably higher than expected (typically log (g) ≈ 1.0–2.0 for supergiants). This discrepancy likely arises from the intrinsic limitations of SED fitting based solely on photometric data, as surface gravity has a relatively weak effect on broadband fluxes. As a result, the procedure may prioritize minimizing residuals over maintaining physical plausibility in log (g).

To address this limitation and assess the validity of the derived log (g) values, we strongly recommend additional high-resolution spectroscopic observations and line-profile analysis. Spectroscopic diagnostics are more sensitive to gravity-dependent features and offer a direct, independent means of constraining surface gravity. Incorporating such constraints would substantially improve the physical reliability and consistency of the derived parameters, ensuring better alignment with the evolutionary status of the stars.

3 Results and discussion

This study focused on determining the physical parameters of 16 hot supergiants by constructing and analyzing their SED across a broad wavelength range, extending from the ultraviolet to the far-infrared. Using a model-fitting procedure that incorporates interstellar extinction, we derived updated estimates of effective temperature Teff, surface gravity log(g), and extinction interstellar A_V for each target star. These parameters are summarized in Table 1, and representative comparisons between the dereddened observed SEDs and the best-fitting models are shown in Figure 1.

Table 1 – Physical parameters of the supergiants in the sample.

Star name	Teff [K]	log(g)	Av	σ
HD 87737	9 500	2.00	0.13	0.185
HD 46300	9 500	2.00	0.17	0.048
BD+60_2582	14 000	2.50	3.06	0.060
HD 5776	11 000	3.50	1.88	0.028
BD+61 153	10 750	3.50	2.89	0.027
HD 161695	9 750	2.00	0.20	0.040
HD 175687	9 500	2.00	0.63	0.051
HD 16778	10 250	2.00	3.07	0.040
HD 202850	11 000	2.00	0.67	0.093
HD 40589	11 750	2.00	1.14	0.087
HD 46769	12 250	3.00	0.22	0.047
HD 59612	7 000	2.00	0.07	0.064
HD 67456	8 750	3.00	0.31	0.034
HD 71833	12 000	3.00	0.08	0.035
HD 35600	10 750	2.00	0.87	0.072
HD 212593	10 750	2.00	0.48	0.055

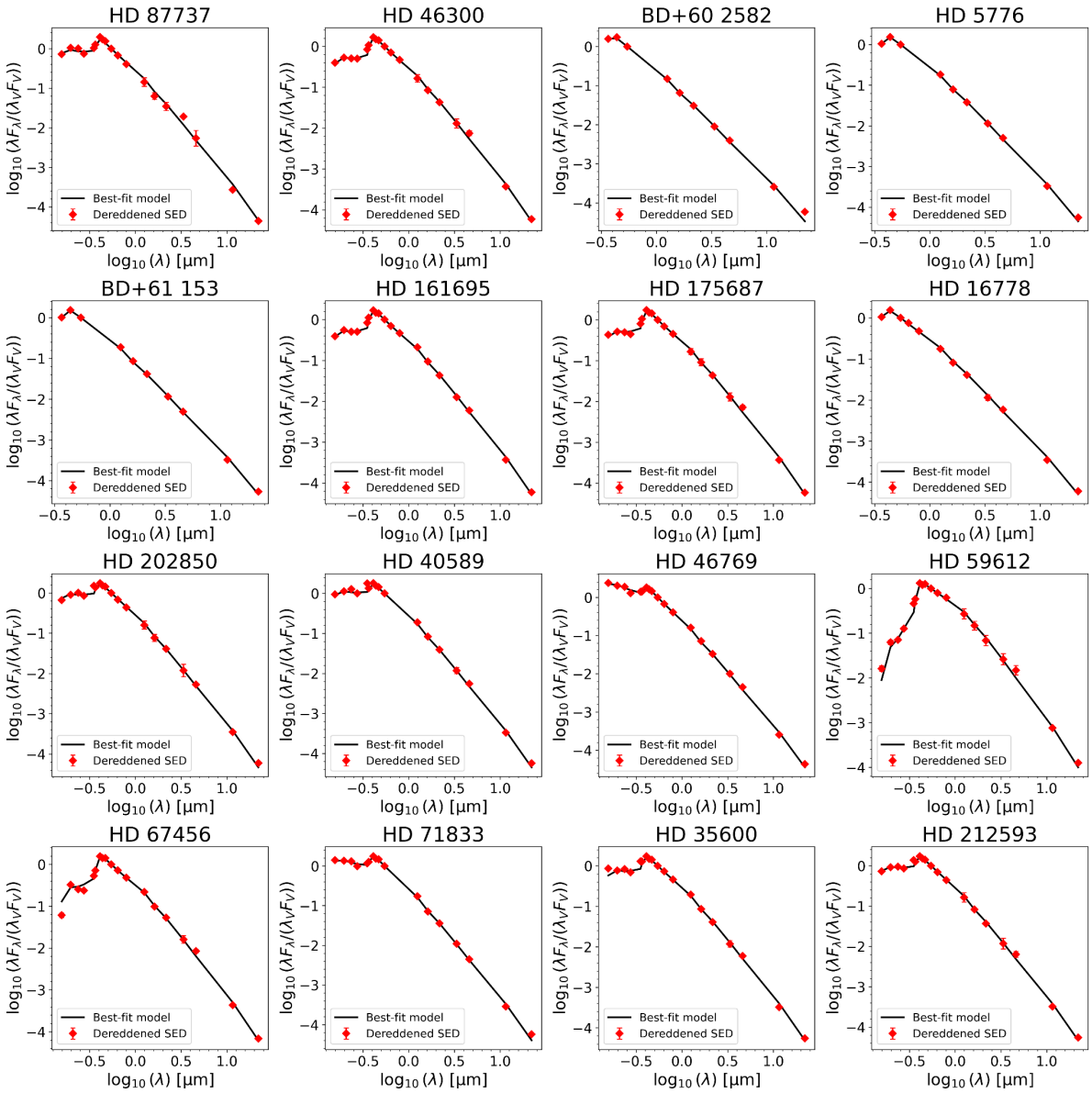

Figure 1 – Comparison between observed and modeled spectral energy distributions for a sample of 16 supergiant stars. The black solid lines represent the best-fitting model SEDs, normalized to the V-band flux. The red diamonds indicate the observed photometric data points, corrected for interstellar extinction and shown with corresponding observational uncertainties. Both axes are plotted on a logarithmic scale.

For most stars, the observed SEDs are well reproduced by the atmospheric models of Castelli & Kurucz, with residuals generally remaining within the expected photometric uncertainties. The good agreement between our results and literature values (as reviewed in the corresponding section) further validates the reliability of the SED-fitting approach. For well-studied supergiants such as HD 87737 and HD 46300 our determinations of Teff, and log(g) agree well with those obtained via high-resolution spectroscopy and spectrophotometry. This confirms that SED analysis, when based on high-quality multi-band photometry and robust extinction modeling, provides a reliable approach to estimate stellar parameters.

In some cases, the shape of the observed SED can offer valuable clues about the star's surrounding environment. A sharp drop in flux in the optical and ultraviolet regions, for instance, often points to strong interstellar extinction and may require a higher A_V value to accurately match the model. On the other hand, an unexpected rise in infrared flux –

especially in the WISE or IRAS bands – may hint at the presence of circumstellar dust, such as disks or extended shells that absorb stellar light and re-emit it at longer wavelengths. Such features typically reveal themselves as systematic deviations from the model fit and may serve as indirect evidence of dust in the immediate vicinity of the star.

The method also proved robust even when only partial photometric coverage was available. The robustness of the fitting procedure is ensured by a grid-search algorithm over a broad parameter space, using multi-band photometry from UV to IR, which allows convergence even when several photometric points are missing or uncertain. The normalization and extinction-fitting procedures enabled the derivation of reliable stellar parameters, despite gaps in some wavelength regions.

Comparing derived results of fundamental parameters with several previous investigations (Table 2), it is clear that the resulting parameters show good agreement with those published in the literature, confirming the reliability of our approach. The SED-method was never used before to determine parameters of these stars, and our investigation clearly shows that it may be used in future.

In summary, the results confirm that SED fitting is a reliable and effective technique for determining the fundamental parameters of hot supergiants. Moreover, it offers a way to identify secondary signatures such as infrared excess, which may indicate mass loss or circumstellar material. The derived parameters can be used to update stellar evolution models, improve distance estimates, and characterize stellar environments. This methodology is well-suited for extension to larger samples and could be integrated into automated pipelines for next-generation photometric surveys.

Table 2 – Comparison between fundamental parameters derived in this paper with the previous ones. *E(B–V) converted using the formula $A_V = 3.1E(B–V)$ [43].

Name	Research	Teff [K]	log g	AV
HD 87737	This paper	9 500	2.00	0.13
	Venn, 1995 [3]	9 700	2.0	
	Przybilla & Butler, 2001 [12]	9 600 ± 150	2.00 ± 0.15	
	Cenarro, 2007 [13]	9 730	1.97	
	Zorec, 2009 [14]	9 820 ± 340		0.16 *
	Firnstein & Przybilla, 2012 [1]	9 600 ± 200	2.05 ± 0.10	0.06 ± 0.06 *
HD 46300	This paper	9 500	2.00	0.17
	Schmidt-Kaler, 1982 [16]	9 730		
	Venn, 1995 [3]	9 700	2.1	
	Verdugo, 1999 [2]	9 750	2.0	
	Zorec, 2009 [14]	9 800 ± 340		0.26 *
	Firnstein & Przybilla, 2012 [1]	11 000 ± 200	2.15 ± 0.10	0.22 ± 0.06 *
BD+60 2582	This paper	14 000	2.50	3.06
	Humphreys, 1978 [17]			2.34
	Firnstein & Przybilla, 2012 [1]	11 900 ± 200	1.85 ± 0.10	2.64 ± 0.06 *
HD 5776	This paper	11 000	3.50	1.88
	Humphreys, 1978 [17]			1.53
	Schmidt-Kaler, 1982 [16]	9 730		
	Garmany & Stencel, 1992 [18]	10 715		
	Verdugo, 1999 [2]	9 500	1.0	
BD+61 153	This paper	10 750	3.50	2.89
	Humphreys, 1978 [17]			2.49
	Schmidt-Kaler, 1982 [16]	9 730		

Continuation of the table

	Verdugo, 1999 [2]	9 750	1.5	
HD 161695	This paper	9 750	2.00	0.20
	Cenarro, 2007 [13]	9 950	2.2	
HD 175687	This paper	9 500	2.00	0.63
	Venn, 1995 [3]	9 400	2.3	
HD 16778	This paper	10 250	2.00	3.07
	Garmany & Stencel, 1992 [18]	9 550		
	Verdugo, 1999 [2]	9 080		
HD 202850	This paper	11 000	2.00	0.67
	Wegner, 2002 [20]			0.40 *
	Markova & Puls, 2008 [19]	11 000	1.87	
	Zorec, 2009 [14]	11 170 ± 450		0.62 *
	Firnstein & Przybilla, 2012 [1]	10 800 ± 200	1.85 ± 0.10	0.40 *
HD 40589	This paper	11 750	2.00	1.14
	Goranova, 2002 [21]	12 000	1.8	
	Zorec, 2009 [14]	11 660 ± 490		
	Samedov, 2023 [22]	10 750 ± 150	1.65 ± 0.2	
HD 46769	This paper	12 250	3.00	0.22
	Lefever, 2007 [23]	12 000	2.57	
	Zorec, 2009 [14]	13 920 ± 710		0.47 *
	Aerts, 2013 [24]	13 000 ± 1000	2.7 ± 0.1	
HD 59612	This paper	7 000	2.00	0.07
	Schmidt-Kaler, 1982 [16]	8 510		
	Venn, 1995 [3]	8 100	1.45	
	Verdugo, 1999 [2]	8 500	1.5	
	Cenarro, 2007 [13]	8 330	1.45	
	Lyubimkov, 2010 [25]	8 620 ± 200	1.78	
HD 67456	This paper	8 750	3.00	0.31
	Przybylski, 1972 [26]	9 500	1.2	
	Venn, 1995 [3]	8 300	2.5	
HD 71833	This paper	12 000	3.00	0.08
	Makaganiuk, 2011 [27]	12 985		
HD 35600	This paper	10 750	2.00	0.87
	Goranova, 2002 [21]	11 000	1.9	
HD 212593	This paper	10 750	2.00	0.48
	Schmidt-Kaler, 1982 [16]	10 300		
	Verdugo, 1999 [2]	10 000	1.5	
	Yuece, 2005 [30]	10 350	1.92	
	Markova & Puls, 2008 [19]	11 800	2.19	
	Zorec, 2009 [14]	11 150 ± 440		
	Firnstein & Przybilla, 2012 [1]	11 200 ± 200	2.10 ± 0.10	0.53 ± 0.06 *
	Wang, 2015 [31]			0.37 *

4 Conclusion

The primary aim of this study was to determine the fundamental parameters of hot supergiants of spectral types B and A through the construction and analysis of SED. The research objectives encompassed the compilation of multiwavelength photometric data, the standardization and conversion of stellar magnitudes into physical fluxes, the construction of SEDs, and their comparison with synthetic photometry derived from model stellar spectra. For this purpose, we employed modern computational techniques, utilized a variety of astronomical databases, and developed specialized software based on the Castelli & Kurucz atmospheric models.

As a result, SEDs were constructed for a sample of 16 stars, and their effective temperatures, surface gravities, and interstellar extinction values were derived. In most cases, the obtained parameters are in good agreement with previously published data, thereby validating the accuracy and robustness of our methodology. For several objects, we identified an excess in the infrared domain, which may indicate the presence of circumstellar dust environments and warrants further spectroscopic and photometric investigation. In some instances, discrepancies between observed and modeled data highlight the need for refinement in the current grid of theoretical models and support the importance of enlarging the stellar sample for improved statistical reliability.

Overall, this study demonstrates the effectiveness of SED analysis as a reliable technique for constraining the physical properties of hot supergiants. The derived results contribute to a more systematic and consistent understanding of evolved massive stars and provide a foundation for future studies involving the calibration of stellar evolutionary models and the investigation of circumstellar phenomena. Looking forward, the methodology presented here can be adapted to larger and more diverse stellar samples and can potentially be integrated with machine learning approaches to enable automated processing of photometric data in next-generation astronomical surveys. To make this approach suitable for large-scale automated applications, a few improvements are needed. These include automatic loading and preparation of photometric data from catalogs, reliable ways to identify and exclude outliers, and the use of prior knowledge – for example, typical log(g) values for different spectral types – to avoid unrealistic solutions. It would also be important to add tools that can estimate uncertainties in the results, such as Bayesian methods.

In addition to these practical improvements, the physical parameters obtained in this study can also help inform models of stellar evolution. Although the focus here was on methodology, the results provide more accurate observational constraints for hot supergiants – an important step toward improving evolutionary tracks and deepening our understanding of how massive stars evolve beyond the main sequence. The precise values of T_{eff} and log(g) allow for more accurate determinations of star's luminosity, radius, and mass, which are fundamental to understanding the internal processes of stars as they evolve through different phases. Thus, these observational constraints serve as valuable benchmarks for testing and calibrating theoretical stellar evolutionary models.

Acknowledgements. This research was funded by the Science Committee of the Ministry of Science and Higher Education of the Republic of Kazakhstan (Grant No. AP23484898).

References

1. Firnstein M., Przybilla N. Quantitative Spectroscopy of Galactic BA-type supergiants. I. Atmospheric parameters // Astronomy & Astrophysics. – 2012, – Vol. 543. A. 80. – P. 17. https://doi.org/10.1051/0004-6361/201219034
2. Verdugo E., Talavera A., Gómez de Castro A. Understanding A-type supergiants II. Atmospheric parameters and rotational velocities of Galactic A-type supergiants // Astronomy & Astrophysics. – 1999. – Vol. 346. – P. 819-830. https://ui.adsabs.harvard.edu/abs/1999A&A...346..819V
3. Venn K. A. Atmospheric Parameters and LTE abundances for 22 galactic, A-type supergiants // The Astrophysical Journal Supplement Series. – 1995. – Vol. 99. – P. 659-692. https://doi.org/10.1086/192201
4. Wolf B. The atmosphere of the A0 Ib supergiant eta Leonis // Astronomy & Astrophysics. – 1971. – Vol. 10. – P. 383-400. https://ui.adsabs.harvard.edu/abs/1971A%26A....10..383W
5. Böhm-Vitense E. Effective temperatures of A and F stars // The Astrophysical Journal. – 1982. – Vol. 255. – P. 191-199. https://doi.org/10.1086/159817

6. Underhill A., Doazan V. B Stars with and without emission lines // NASA SP-456. – 1982. – Vol. 57. – P. 485. https://ui.adsabs.harvard.edu/abs/1982bsww.book.....U

7. Lambert D., Hinkle K. H., Luck R. E. The peculiar supergiant HR 4049 // The Astrophysical Journal. – 1988. – Vol. 333. – P. 917-924. https://doi.org/10.1086/166800

8. Lobel A., Achmad L, de Jager C., Nieuwehnuijzen H. Atmospheric model and dynamical state of the atmosphere of the supergiant Eta Leonis (A0Ib) // Astronomy & Astrophysics. – 1992. – Vol. 256. – P. 159-165. https://ui.adsabs.harvard.edu/abs/1992A&A...256..159L

9. Venn K. A. CNO abundances and the evolutionary status of three A-type supergiants // The Astrophysical Journal. – 1993. – Vol. 414. – P. 316-332. https://ui.adsabs.harvard.edu/abs/1993ApJ...414..316V

10. Przybylski A. The analysis of the low gravity halo star HD 214539 // MNRAS. – 1969. – Vol. 146. – P. 71-90. https://doi.org/10.1093/mnras/146.1.71

11. Boyarchuk A. A. A quantitative analysis of the chemical composition of the atmosphere of the bright component of β – Lyrae // Soviet Astronomy. – 1959. – Vol. 3. – P. 748-758. https://ui.adsabs.harvard.edu/abs/1959SvA.....3..748B

12. Przybilla N., Butler K. Non-LTE line formation for N I/II: Abundances and stellar parameters. Model atom and first results on BA-type stars // Astronomy & Astrophysics. – 2001. – Vol. 379. – P. 955-975. https://doi.org/10.1051/0004-6361:20011393

13. Cenarro A. J., Peletier R. F., Sánchez-Blázquez P. et al. Medium-resolution Isaac Newton Telescope library of empirical spectra – II. The stellar atmospheric parameters // MNRAS. – 2007. – Vol. 374. – P. 664-690. https://doi.org/10.1111/j.1365-2966.2006.11196.x

14. Zorec J., Cidale L., Arias M. L. et al. Fundamental parameters of B supergiants from the BCD system. I. Calibration of the (λ_1, D) parameters into T_{eff} // Astronomy & Astrophysics. – 2009. – Vol. 501. – P. 297-320. https://doi.org/10.1051/0004-6361/200811147

15. Przybilla N., Firnstein M., Nieva M. F., Meynet G., Maeder A. Mixing of CNO-cycled matter in massive stars // Astronomy & Astrophysics. – 2010, – Vol. 517. – A. 38. – P. 6. https://doi.org/10.1051/0004-6361/201014164

16. Schmidt-Kaler Th. 4.1.4 Effective temperatures, bolometric corrections and luminosities // Landolt-Boernstein – Group VI Astronomy and Astrophysics. – 1982. – Vol. 2. – SubVol. B. – P. 455. https://doi.org/10.1007/b20014

17. Humphreys R. M. Studies of luminous stars in nearby galaxies. I. Supergiants and O stars in the Milky Way // The Astrophysical Journal Supplement Series. – 1978. – Vol. 38. – P. 309-350. https://ui.adsabs.harvard.edu/abs/1978ApJS...38..309H

18. Garmany C. D., Stencel R. E. Galactic OB associations in the northern Milky Way galaxy. I. Longitudes 55 to 150 // Astronomy & Astrophysics Supplement Series. – 1992. – Vol. 94. – P. 211-244. https://ui.adsabs.harvard.edu/abs/1992A&AS...94..211G

19. Markova N., Puls J. Bright OB stars in the galaxy. IV. Stellar and wind parameters of early to late B supergiants // Astronomy & Astrophysics. – 2008. – Vol. 478. – P. 823-842. https://doi.org/10.1051/0004-6361:20077919

20. Wegner W. Atlas of interstellar extinction curves of OB stars covering the whole available wavelength range // Baltic Astronomy. – 2002. – Vol. 11. – P. 1-74. https://ui.adsabs.harvard.edu/abs/2002BaltA..11....1W

21. Goranova Yu.; Georgiev Ts., Iliev L. et al. Radial velocities of B-stars towards the galactic anti-center // Publ. Astron. Obs. Belgrade. – 2002. – Vol. 73. – P. 153-157. https://www.researchgate.net/publication/253486235

22. Samedov Z. A., Rustem U. R., Hajiyeva G. M., Aliyeva Z. F. Fundamental parameters of supergiant star HD 40589 (A0Iab) // Odessa Astronomical publications. – 2023. – Vol. 36. – P. 86-87. https://doi.org/10.18524/1810-4215.2023.36.290802

23. Lefever K., Puls J., Aerts C. Statistical properties of a sample of periodically variable B-type supergiants. Evidence for opacity-driven gravity-mode oscillations // Astronomy & Astrophysics. – 2007. – Vol. 463. – P. 1093-1109. https://doi.org/10.1051/0004-6361:20066038

24. Aerts C., Simón-Díaz S., Catala C. et al. Low-amplitude rotational modulation rather than pulsations in the CoRoT B-type supergiant HD 46769 // Astronomy & Astrophysics. – 2013. – Vol. 557. – A. 114. – P. 9. https://doi.org/10.1051/0004-6361/201322097

25. Lyubimkov L. S., Lambert D. L., Rostopchin S. I. et al. Accurate fundamental parameters for A, F, and G-type supergiants in the solar neighbourhood (Paper I) // MNRAS. – 2010. – Vol. 402. – P. 12. https://doi.org/10.1111/j.1365-2966.2009.15979.x

26. Przybylski A. The analysis of the small magellanic cloud supergiant HD 7583 // MNRAS. – 1972. – Vol. 159. – P. 155-163.https://doi.org/10.1093/mnras/159.2.155

27. Makaganiuk V., Kochukhov O., Piskunov N. et al. The search for magnetic fields in mercury-manganese stars // Astronomy & Astrophysics. – 2011. – Vol. 525. – A. 97. – P. 275-284. https://doi.org/10.1051/0004-6361/201015666

28. Moon T. T., Dworetsky M. M. Grids for the determination of effective temperature and surface gravity of B, A and F stars using *uvby*β photometry // MNRAS. – 1985. – Vol. 217. – P. 305-315. https://doi.org/10.1093/mnras/217.2.305

29. Takeda Y., Takada-Hidai M. Helium and carbon abundances in late-B and early-A supergiants // Publications of the Astronomical Society of Japan. – 2000. – Vol. 52. – P. 113-125. https://ui.adsabs.harvard.edu/abs/2000PASJ...52..113T

30. Yüce K. Spectral analysis of 4 Lacertae and ν Cephei // Baltic Astronomy. – 2005. – Vol. 14. – P. 51-82. https://ui.adsabs.harvard.edu/abs/2005BaltA..14...51Y

31. Wang X., Hummel C. A., Ren S. et al. The three-dimensional orbit and physical parameters of 47 Oph // The Astronomical Journal. – 2015. – Vol. 149:110. – P. 7. https://doi.org/10.1088/0004-6256/149/3/110

32. Lorenzo-Gutiérrez A., Alfaro E. J., Maíz-Apellániz J. et al. Deriving stellar parameters from GALANTE photometry: bias and precision // MNRAS. – 2020. – Vol. 494. – P. 3342-3357. https://doi.org/10.1093/mnras/staa892

33. Ochsenbein F., Bauer P., Marcout J. The VizieR database of astronomical catalogues // Astronomy and Astrophysics Supplement Series. – 2000. – Vol. 143(1). – P. 23-32. https://doi.org/10.1051/aas:2000169

34. Mermilliod J.-C., Hauck B., Mermilliod M. The general catalogue of photometric data (GCPD). II // Astronomy and Astrophysics Supplement Series. – 1997. – Vol. 124(2). – P. 349-352. https://doi.org/10.1051/aas:1997197

35. Thompson G. I., Nandy K., Jamar C. et al. Catalogue of stellar ultraviolet fluxes from the TD-1 Satellite // ESRO SP-56, European Space Research Organisation. – 1978. – P. 295. https://ui.adsabs.harvard.edu/abs/1978csuf.book.....T

36. Lanz T. Photoelectric photometric catalogue in the Johnson *UBVRI* system // Astronomy & Astrophysics Supplement Series. – 1986. – Vol. 65. – P. 195-197. https://ui.adsabs.harvard.edu/abs/1986A%26AS...65..195L

37. Hauck B., Mermilliod M. *uvbyβ* photoelectric photometric catalogue, 1953-1996 // Astronomy and Astrophysics Supplement Series. – 1998. – Vol. 129. – P. 431-433. https://doi.org/10.1051/aas:1998195

38. Paunzen E. A new catalogue of Strömgren-Crawford *uvbyβ* photometry // Astronomy and Astrophysics. – 2015. – Vol. 580. – A. 23. https://doi.org/10.1051/0004-6361/201526413

39. Skrutskie M. F., Cutri R. M., Stiening R. et al. The two micron all sky survey (2MASS) // Astronomical Journal. – 2006. – Vol. 131(2). – P. 1163-1183. https://doi.org/10.1086/498708

40. Gezari D. Y., Schmitz M., Pitts P. S. Catalog of infrared observations. 5th edition // NASA RP-1294. – 1999. – P. 384. https://ui.adsabs.harvard.edu/abs/1999yCat.2225....0G

41. Wright E. L., Eisenhardt P. R. M., Mainzer A. K. et al. The wide-field infrared survey explorer (WISE) Mission // Astronomical Journal. – 2010. – Vol. 140(6). – P. 1868-1881. https://doi.org/10.1088/0004-6256/140/6/1868

42. Castelli F., Kurucz R. L. New grids of ATLAS9 model atmospheres // IAU Symp. No 210, Modeling of Stellar Atmospheres. – 2003. – A. 20. https://doi.org/10.48550/arXiv.astro-ph/0405087

43. Cardelli J. A., Clayton G. C., Mathis J. S. The relationship between infrared, optical, and ultraviolet extinction // The Astrophysical Journal. – 1989. – Vol. 345. – P. 245-256. https://doi.org/10.1086/167900

Information about authors:

Alina Gyuchtash, *BSc in Physics and Astronomy is a Research assistant at the Fesenkov Astrophysical Institute (Almaty, Kazakhstan), e-mail: AlinaGyuchtash@gmail.com*

Shakhida Tashmakhomedovna Nurmakhametova, *BSc in Physics and Astronomy is a Research assistant at the Fesenkov Astrophysical Institute (Almaty, Kazakhstan), e-mail: shahidanurmahametova@gmail.com*

Nadezhda Leonidovna Vaidman, *MSc in Physics and Astronomy* is a *Research associate at the Fesenkov Astrophysical Institute (Almaty, Kazakhstan), e-mail: nva1dmann@gmail.com*

Serik Anatolyevich Khokhlov, *PhD is a Chief Investigator at the Fesenkov Astrophysical Institute (Almaty, Kazakhstan), email: skhokh88@gmail.com*

Aldiyar Talgatovich Agishev, PhD is a Senior researcher at the Fesenkov Astrophysical Institute, (Almaty, Kazakhstan), e-mail: aldiyar.agishev@gmail.com

Aigerim Bakhytkyzy, MSc is a Visiting Scholar at the Department of Physics and Astronomy, University of North Carolina – Greensboro (Greensboro, USA), e-mail: aigerim423113@gmail.com